THE JOURNAL OF BIOLOGICAL CHEMISTRY VOL. 289, NO. 50, pp. 34990–35002, December 12, 2014

Identification of a Membrane-targeting Domain of the Transient Receptor Potential Canonical (TRPC)4 Channel Unrelated to Its Formation of a Tetrameric Structure*

Received for publication, May 26, 2014, and in revised form, October 17, 2014 Published, JBC Papers in Press, October 27, 2014, DOI 10.1074/jbc.M114.584649

Jongyun Myeong[1,2], **Misun Kwak**[1,2], **Chansik Hong**[2], **Ju-Hong Jeon, and Insuk So**[3]

From the Department of Physiology, Seoul National University College of Medicine

Background: Functional TRPC4/5 channels make tetrameric structures in the plasma membrane.
Results: The 21–30 motif of TRPC4/5 regulates the membrane expression of the channels by interacting with $PI(4,5)P_2$.
Conclusion: The 21–30 motif of TRPC4/5 has an essential role in the membrane expression that does not involve the tetrameric structure.
Significance: Our findings indicate the membrane expression regulating domain of TRP channels.

Canonical transient receptor potential (TRPC) channels are Ca^{2+}-permeable nonselective cation channels that are activated by a wide variety of stimuli, including G protein-coupled receptors (GPCRs). The TRPC4 channel is expressed in a punctate distribution in the membrane. To identify the regulating region of the channel trafficking to the membrane, we generated deletion mutants of the TRPC4 channel. We determined that when either region that was downstream of the 20 amino acids of the N terminus or the 700–730 amino acids was deleted, the mutants were retained in the endoplasmic reticulum. By coexpression of the wild-type TRPC4 with deletion mutants, we found that the 23–29 amino acids of the N terminus regulate a membrane trafficking. Additionally, by the fluorescence resonance energy transfer (FRET) method, we found that the regions downstream of the 99 amino acid region of the N terminus and upstream of the 730 amino acid region in the C terminus produce assembly of the TRPC4 tetramers. We inferred the candidate proteins that regulate or interact with the 23–29 domain of TRPC4.

Transient receptor potential cation channel (TRPC)[4] 4 proteins are composed of four ankyrin-like repeats and a coiled-coil domain in their N terminus strands followed by six transmembrane domains and a C terminus that contains the SESD1, CIRB, and PDZ binding domains. It is well-known that when the TRPC channels are partially deleted or mutated, their trafficking at the plasma membrane is limited, and they are retained in the endoplasmic reticulum (ER) or Golgi (1–4). Among the TRPC channels, TRPC4 and TRPC5 channels are unique in the aspect of their activation by the $G\alpha_i$ protein. Additionally, the region that is responsible for the interaction with $G\alpha_i$ protein is important for CaM binding. The deletion of this region causes the TRPC4 and TRPC5 channel to be nonfunctional (5, 6). When Arg^{718}, Lys^{722}, and Arg^{723} were substituted with alanine, mouse TRPC5 were destroyed and failed respond to stimulation by thrombin and bradykinin in both CHO and HEK293 cells. However, the mutant proteins were efficiently delivered to the plasma membrane when detected by surface biotinylation (6). In this report, we concluded that the calmodulin and inositol 1,4,5-triphosphate receptor-binding (CIRB) region is important for channel gating and/or channel activation by agonists rather than that there is a dysfunction in the trafficking and translocation of the channel protein. Similar results were obtained in the TRPC4 channel expressed in HEK cells (5). One point mutation within the region (N712R) did not show any typical doubly rectifying I-V curve, whereas R716A mutant showed an enhanced basal activity (5). This finding is in contrast to the finding that deletion of the CIRB site impaired the plasma membrane translocation of TRPC3 (3).

When TRPC4 channels were expressed in HEK cells, their distribution was not homogeneous at the plasma membrane, and instead, they existed as puncta or discrete microdomains. Several studies have shown that when the C terminus domain is deleted, the expression of the channels is limited because the deleted region is where the regulation of channel trafficking takes place (7, 8). On the other hand, the importance of the N terminus and C terminus domain with regard to the formation of the TRPC4 multimer has also been studied (9–11). The ankyrin repeat domains are especially important for the assembly of tetrameric TRPC4 structure. Recently, (12) showed the structure of TRPV1, which suggests that ARD was not involved in the assembly of TRPV1 tetramers but instead is involved in protein-protein interactions with other proteins.

In a previous study (5), we investigated the interaction of TRPC4 mutants with $G\alpha_i$ proteins and observed their expression at the plasma membrane. Interestingly, the distribution of

* This study was supported by grants obtained from the National Research Foundation of Korea, which is funded by the Ministry of Science, ICT (Information & Communication Technology) and Future Planning (MSIP) of the Korean government (2010-0019472 and 2012R1A2A1A01003073) (to I. S.).
[1] Both authors contributed equally to this work.
[2] Supported by the graduate program of BK21 and by grants from the MSIP.
[3] To whom correspondence should be addressed: Dept. of Physiology, Seoul National University College of Medicine, Seoul National University Graduate School, Biomedical Science Bldg. 101, 103 daehakro, Jongro-gu, Seoul 110-799, Korea. Tel.: 82-2-740-8228; Fax: 001-82-2-763-9667; E-mail: insuk@snu.ac.kr.
[4] The abbreviations used are: TRPC, transient receptor potential cation channels; PM, plasma membrane; NE, nuclear envelope; FRET, Förster resonance energy transfer; GTPγS, guanosine 5′-3-O-[γ-thio]triphosphate; aa, amino acid; CBS, caveolin binding site; ER, endoplasmic reticulum; CIRB, calmodulin and inositol 1,4,5-triphosphate receptor-binding; CFP, cyan fluorescent protein; YFP, yellow fluorescent protein.

TRPC4 at the plasma membrane depended on the deletion regions. From the deletion mutants, we found that the 23–29 amino acid (aa) domain is important for membrane trafficking and that downstream of 99 aa of the N terminus and 700–730 aa region is important for the assembly of TRPC4 tetramers.

EXPERIMENTAL PROCEDURES

Cell Culture and Transient Transfection, cDNA Clones—Human embryonic kidney (HEK293) cells (ATCC, Manassas, VA) were maintained according to the supplier's recommendations. HEK293 cells were incubated in Dulbecco's Modified Eagle's Medium (DMEM) supplemented with 10% heat-inactivated FBS and penicillin (100 units/ml), streptomycin (100 μg/ml) at 37 °C in 5% CO_2 humidified incubator. Cells were seeded in confocal dish for recording FRET or 12-well plates for whole-cell patch clamp. The following day, transfection was performed with Fugene-6 according to the manufacturer's instructions. XFP (CFP or YFP)-tagged TRPC4, TRPC5, and TRPC1 were transfection in this way. The next day we performed electrophysiology or FRET experiments.

Electrophysiology—The cells were transferred onto a solution chamber on the stage of an invert microscope (IX70, Olympus, Japan). The whole cell configuration was used to measure TRPC channel current in HEK cells as described previously (13–17). Cells were left for 10–15 min to attach to coverslips. Whole cell current were recorded using an Axopatch 200B amplifier (Axon instruments). Patch pipettes were made from bososilicate glass and had resistances of 3–5 MΩ when filled with normal intracellular solutions. Bath solution was changed from Normal Tyrode (NT) to Cs^+ rich external solution after whole cell recording system established. The NT contained 135 mM NaCl, 5 mM KCl, 2 mM $CaCl_2$, 1 mM $MgCl_2$, 10 mM glucose, and 10 mM HEPES with a pH that was adjusted to 7.4 using NaOH. The Cs^+-rich external solution contained equimolar CsCl rather than NaCl and KCl. The internal solution contained 140 mM CsCl, 10 mM HEPES, 0.2 mM Tris-guanosine 5′-triphospate, 0.5 mM EGTA, and 3 mM Mg-adenosine 5′-triphosphate with a pH that was adjusted to 7.3 with CsOH. We used 0.2 mM GTPγS that was purchased from Sigma. Voltage ramp pulse was applied from +100 mV to −100 mV for 500 ms at −60 mV holding potential. Experiments were performed at room temperature (18–22 °C). The recording chamber was continuously perfused at a flow rate of 1–2 ml/min.

Image Quantification and FRET Measurements—HEK293 cells were cultured in 35-mm coverslip bottom dish to obtain image and to measure FRET efficiency. To obtain the image and FRET efficiency of a cell, we used an inverted microscope (IX70, Olympus, Japan) with a 60× oil objective lens and the 3 cube FRET calculation (18) controlled by MetaMorph 7.6 (Molecular Devices). We mainly used 3 cube FRET. 3 cube FRET efficiency (cube settings for CFP, YFP, and Raw FRET) were acquired from a pE-1 Main Unit to 3 cube FRET (excitation, dichroic mirror, filter) through a fixed collimator: CFP (ET 435/20 nm, ET CFP/YFP/mCherry beam splitter, ET 470/24 nm, chroma); YFP (ET500/20m, ET CFP/YFP/mCherry beam splitter, ET535/30 nm, chroma); and Raw FRET (ET435/20 nm, ET CFP/YFP/mCherry beam splitter, ET535/30 nm, Chroma). The excitation LED and filter were sequentially rotated, rotation period for each of filter cubes was ~0.5 s, and all images (three for CFP/YFP/Raw FRET, respectively) were obtained within 1.5 s. Each of the images was acquired on a cooled 10 MHz (14 bit) CCD camera (DR-328G-C01-SIL: Clara, ANDOR Technology) with an exposure time of 100 ms with 2 × 2 or 3 × 3 binning under the control of MetaMorph 7.6 software. Our FRET recording of the fluorophores was restricted in a range of CFP/YFP ratio being 0.5 to 2.0.

FR and FRET Efficiency Computation (18)—FRET Ratio (FR) is equal to the fractional increase in YFP emission due to FRET and was calculated as in Equation 1,

$$FR = \frac{F_{A_D}}{F_A} = \frac{[S_{FRET}(DA) - R_{D1} \cdot S_{CFP}(DA)]}{R_{A1} \cdot [S_{YFP}(DA) - R_{D2} \cdot S_{CFP}(DA)]} \quad \text{(Eq. 1)}$$

S_{CUBE} (SPECIMEN) denotes an intensity measurement, where CUBE indicates the filter cube (CFP, YFP, or FRET) and SPECIMEN indicate whether the cell is expressing donor (D; CFP), acceptor (A; YFP), or both (DA). $R_{D1} = S_{FRET}(D)/S_{CFP}(D)$, $R_{D2} = S_{YFP}(D)/S_{CFP}(D)$, and $R_{A1} = S_{FRET}(A)/S_{YFP}(A)$ are predetermined constants from measurements applied to single cells expressing only CFP- or YFP-tagged molecules. Although three-cube FRET does not require that CFP and YFP fusion constructs preserve the spectral features of the unattached fluorophores, similar ratios and recorded spectra furnished two indications that the spectral features of the fluorophores were largely unperturbed by fusion. Since *FR* relies on YFP emission, YFP should be attached to the presumed limiting moiety in a given interaction. Subsequent quantitative calculations based on *FR* relied on a presumed 1:1 interaction stoichiometry. The effective FRET efficiency (E_{EFF}) was determined by Equation 2,

$$E_{EFF} = E \times A_b = (FR - 1)[E_{YFP}(440)/E_{CFP}(440)] \quad \text{(Eq. 2)}$$

where E is the intrinsic FRET efficiency when fluorophore-tagged molecules are associated with each other, A_b is the fraction of YFP tagged molecules that are associated with CFP-tagged molecules, and the bracketed term is the ratio of YFP and CFP molar extinction coefficients scaled for the FRET cube excitation filter (21). We determined this ratio to be 0.094 based on maximal extinction coefficients for ECFP and EYFP (19) and excitation spectra measured in our laboratory. FRET was also assessed by measuring dequenching of donor emission following nearly complete acceptor photodestruction (20) by 30 min of strong illumination through a 540AF30 excitation filter. This spared the CFP chromophore in control experiments. Here, the effective FRET efficiency is calculated as Equation 3,

$$E_{EFF} = E \times D_b = [1 - S_{CFP}(DA)_{before}/S_{CFP}(DA)_{after}] \quad \text{(Eq. 3)}$$

where $S_{CFP}(DA)_{before}$ and $S_{CFP}(DA)_{after}$ are CFP emission prior to and following YFP photobleaching, and *D*b is the fraction of CFP-tagged molecules that are associated with YFP-tagged molecules (21).

Western Blotting Analyses, Co-IP, and Surface Biotinylation—For Western blotting, cells were seeded in 6-well plates. On the next day, 0.5–2 μg/well of TRPC4β cDNA was transfected into

cells using the transfection reagent Lipofectamine 2000 (Invitrogen) according to the manufacturer's protocol. After transfection for 24 h, the cells were harvested as follows. Lysates were prepared in lysis buffer (0.5% Triton X-100, 50 Tris-Cl, 150 NaCl, 1 EDTA, pH 7.5, (in mM)) by being passed through a 26-gauge needle 7–10 times after sonication. Lysates were centrifuged at 13,000 × *g* for 10 min at 4 °C, and the protein concentration in the supernatants was determined. The proteins extracted in sample buffer were loaded onto 8% Tris-glycine SDS-PAGE gels, and then subsequently transferred onto a PVDF membrane. The proteins were probed with GFP (Invitrogen) or β-Actin (GeneTex) antibodies for GFP-tagged or housekeeping protein as indicated.

Surface Biotinylation—PBS-washed cells were incubated in 0.5 mg/ml sulfo-NHS-LC-biotin (Pierce) in PBS for 30 min on ice. Afterward, the biotin was quenched by the addition of 100 mM glycine in PBS. The cells were then processed as described above to make cell extract. Forty microliters of 1:1 slurry of immobilized avidin beads (Pierce) were added to 300 μl of cell lysates (500 μg of protein). After incubation for 1 h at room temperature, beads were washed three times with 0.5% Triton-X-100 in PBS, and proteins were extracted in sample buffer. Collected proteins were then analyzed by Western blot. The experiment was performed as previously described in detail (22).

Measurement of Colocalization and Quantification in Images—To determine colocalization of two image in membrane of cell, we made a binary mask image using the "image threshold" routine of MetaMorph 7.6. A CFP mask and a YFP mask were made from a CFP image and a YFP image, respectively. We defined the overlapping area of the CFP mask and the YFP mask as the colocalization region. Finally, the colocalization was calculated by dividing the spatially area of colocalization region over the CFP masked area.

To determine the quantification of membrane expression in image, we substrate background intensity from original image using the "Background subtraction" routine of MetaMorph 7.6. We obtained plasma membrane region from the PH-YFP image expressing membrane region. Then we obtained intensity of membrane region defined by PH-YFP image and total intensity whole cell region. Finally, the membrane/total ration was calculated by dividing the membrane intensity over the total intensity.

RESULTS

Membrane Expression of TRPC4 Deletion Mutants—It has been suggested that the TRPC channels assemble into tetramers, and the expression of the wild type (WT) TRPC4 (TRPC4-WT) channel shows a punctate distribution at the plasma membrane (PM) (23). However, some of the deletion mutants of the TRP channels, namely, TRPV4 (4), TRPC3 (3), TRPV5, 6 (2), TRPM4 (1), and TRPV5 (24), have restricted translocation to the PM and appeared to be predominantly located in the intracellular compartments, for example, the endoplasmic reticulum. Previous reports have shown that because the C terminus region of TRPC4 regulates the insertion of the channel into the PM, the deletion of certain C terminus regions restricts trafficking the channel proteins at the PM (7, 25). We generated deletion mutants of TRPC4β to find regions that regulate the expression of the channel at the PM and its function (Fig. 1*A*).

To observe the subcellular localization of TRPC4β deletion mutants, the constructs of CFP- or YFP-tagged PLCδ PH domain as a membrane marker were co-expressed in HEK293 cells (Fig. 1*B*). Red and green represent CFP and YFP in all of the images. The PH domain of PLCδ binds specifically to PIP_2 at the PM (26). The TRPC4-WT channel is at the PM in the manner of a punctate distribution. To find the domain that is crucial for the expression of the TRPC4 channel at the PM, we checked a deletion mutant distribution in the HEK293 cells.

Fig. 1*B* shows that the TRPC4-WT channel and N terminus deletion mutants TRPC4-Δ1–10 and TRPC4-Δ11–20 manifested a robust punctate distribution at the cell surface, whereas TRPC4-Δ21–30, TRPC4-Δ1–30, TRPC4-Δ11–30, TRPC4-Δ1–98, and TRPC4-Δ1–124 showed retention in the cytosol. When the C terminus deletion mutants were observed, the CIRB domain and SESTD1-deleted mutants (TRPC4-Δ700–728, TRPC4-Δ700–710, and TRPC4-Δ710–720) were not expressed at the PM and were instead retained in the cytosol. Interestingly, the deletion mutant, in which 150 aa were deleted in the C terminus (TRPC4-Δ720–870), was expressed at the plasma membrane at a similar expression level as TRPC4-WT. A line scan across the image showed similar results (Fig. 1*B*). To quantify the surface expression of the mutants, the intensity of surface-expressed fluorescence in the image divided by the total intensity of the whole cell is shown (Fig. 1*C*).

To study whether the mutants expressed in the cytosol were retained in the endoplasmic reticulum, GFP variant-tagged calnexin, an ER-resident chaperon, was co-expressed. In contrast to TRPC4β-WT, deletion mutants expressed in the cytosol (TRPC4β-Δ21–30, TRPC4β-Δ1–30, TRPC4β-Δ11–30, TRPC4β-Δ1–98, TRPC4β-Δ1–124, TRPC4β-Δ700–728, TRPC4β-Δ700–710, and TRPC4β-Δ710–720) were co-localized with fluorescence-tagged calnexin (Fig. 2*A*).

To confirm the surface expression quantitatively with a biochemical experiment, we used cell surface biotinylation (Fig. 2*B*). TRPC4 and deletion mutant expression in whole cell lysate and the biotinylated fraction were determined using immunoblotting. Strikingly, both TRPC4β-WT and TRPC4β-Δ21–30 were present at the plasma membrane, although the latter is significantly reduced (30.76 ± 10.23%, $n = 3$) at the PM. This finding was confirmed by quantification of the protein levels (Fig. 2*B*).The activity of the deletion mutants was measured by the TRPC4 current in the deletion mutants in response to GTPγS, which is a well-known activator of TRPC4 (Fig. 2*C*). TRPC4β-WT, TRPC4β-Δ1–10, TRPC4β-Δ11–20, and TRPC4β-Δ720–870 showed the typical TRPC4 current with a double rectifying shape that is a general shape of the I/V shape of TRPC4. On the other hand, other mutants did not show typical TRPC4 currents. We also generated a mutant that lacks the last 4 C terminus aa (TTRL) that comprise a PDZ domain-binding motif. This motif binds to the PDZ domain of the scaffolding proteins EBP50 and ZO-1 and regulates the surface expression of TRPC4 (7, 25). In contrast to the previous results, we could not find a difference between the membrane expression and the function of TRPC4β-ΔTTRL and TRPC4-WT (Fig. 2*D*).

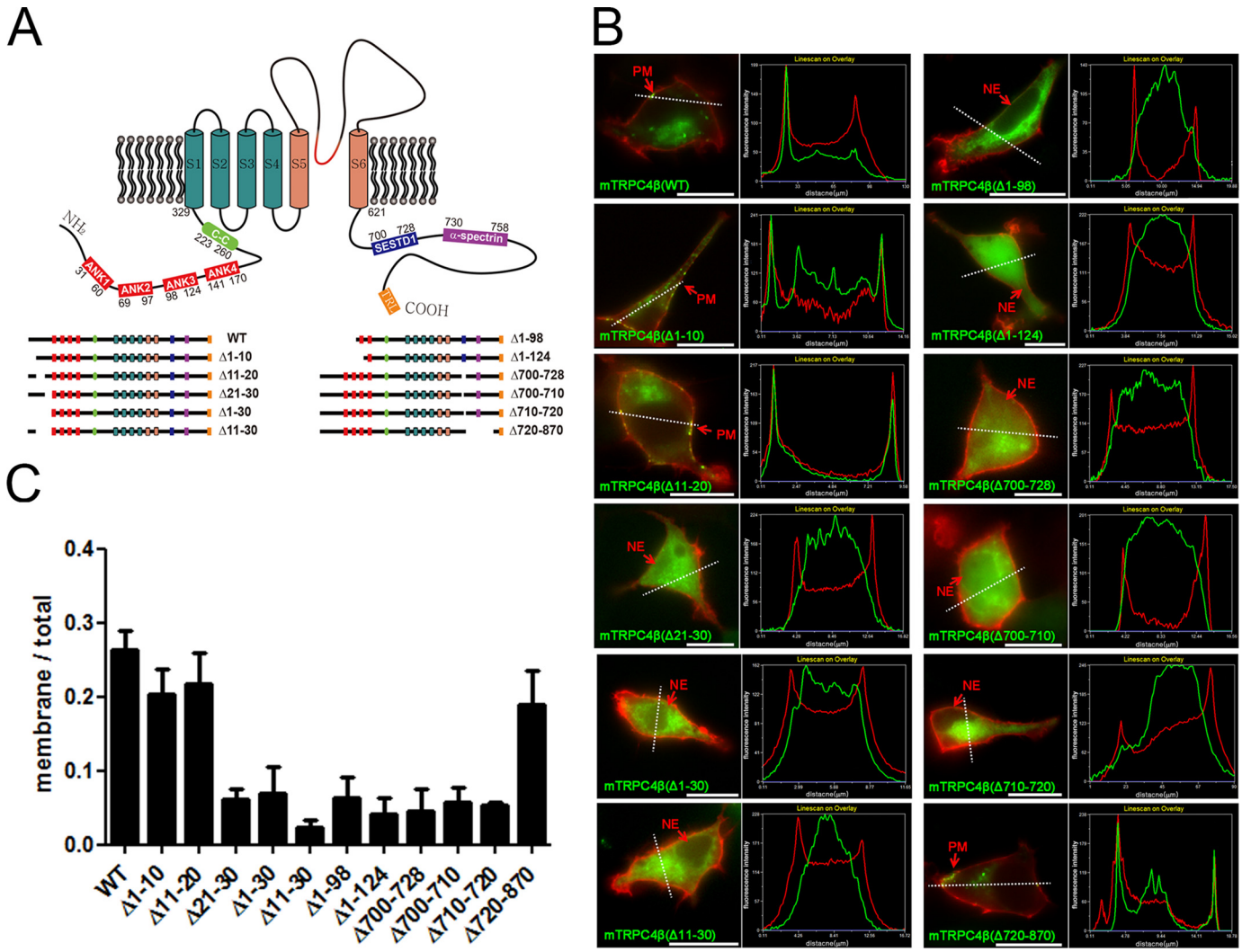

FIGURE 1. **Membrane expression of TRPC4 deletion mutants.** *A*, diagram of deletion mutants of TRPC4β. The TRPC4 protein has four ankyrin-like repeats and a coiled-coil domain in their N terminus strands followed by six transmembrane domains and a C terminus that contains the SESD1, CIRB, and PDZ binding domain. *B*, CFP-tagged deletion mutants of TRPC4β (*green*) were coexpressed with the PH-YFP (*red*), selectively binding to PI(4,5)P_2, as an indicator of plasma membrane in HEK293 cells. Wild type TRPC4β channel, Δ1–10, Δ11–20, and Δ720–870 deletion mutants were observed in the plasma membrane of the cells. The scale bar represents 10 μm. The line scan shows CFP-tagged mutants and PH-YFP intensity followed by a *white dashed line*. *C*, quantification of the membrane expression of the mutants. This graph shows the fluorescence intensity ratio of the membrane expression of deletion mutants to the whole cell expression. Error bars indicate S.E.

These results suggest that there is a correlation between the whole cell current and punctate distribution at the PM of the TRPC4 channel and between trafficking into the plasma membrane (surface biotinylation) and the punctate distribution at the PM of the TRPC4 channel, except for TRPC4-Δ1–10.

Regions of TRPC4 for the Punctate Distribution at the Plasma Membrane—In the experiments mentioned above, the mutants might be retained in the ER due to either a lack of the region for membrane anchoring or impaired tetrameric assembly. A functional TRPC channel complex is believed to be composed of a tetrameric structure of TRPC proteins. Thus, we can infer that TRPC4-WT might rescue TRPC4 deletion mutants that do not have the membrane anchoring region by making tetramers. To test whether TRPC4-WT could rescue deletion mutants that are retained in the endoplasmic reticulum, we co-expressed TRPC4β-WT-YFP and CFP-fused deletion mutants of TRPC4β in HEK293 cells and visualized the subcellular distribution by microscopy. As shown in Fig. 3*A*, the TRPC4β-WT-YFP at the plasma membrane overlapped only in cells that expressed TRPC4β-WT-CFP, TRPC4-Δ1–10-CFP, Δ11–20-CFP, Δ21–30-CFP, Δ1–30-CFP, Δ11–30-CFP, Δ1–98-CFP, and Δ720–870-CFP, whereas retention in the cytosol was detected in the other mutants. We observed that TRPC4-WT is capable of ushering TRPC4β-Δ21–30, TRPC4β-Δ1–30, TRPC4β-Δ11–30, and TRPC4β-Δ1–98 into the plasma membrane, most likely by forming mixed tetramers. A line scan across the image showed similar results (Fig. 3*A*). We quantified the PM distribution of mutants when co-expressed with the wild type channel or when expressed alone (Fig. 3*B*), and we measured the colocalization of the wild type TRPC4 with deletion mutants at the plasma membrane (Fig. 3*C*). Fig. 3*C* shows the overlapping region of wild type TRPC4 with deletion mutants at the PM of the cell. This result indicates that some deletion mutants can be inserted into the PM when co-expressed with wild type TRPC4, whereas when expressed alone, they are retained in the endoplasmic reticulum. This result also

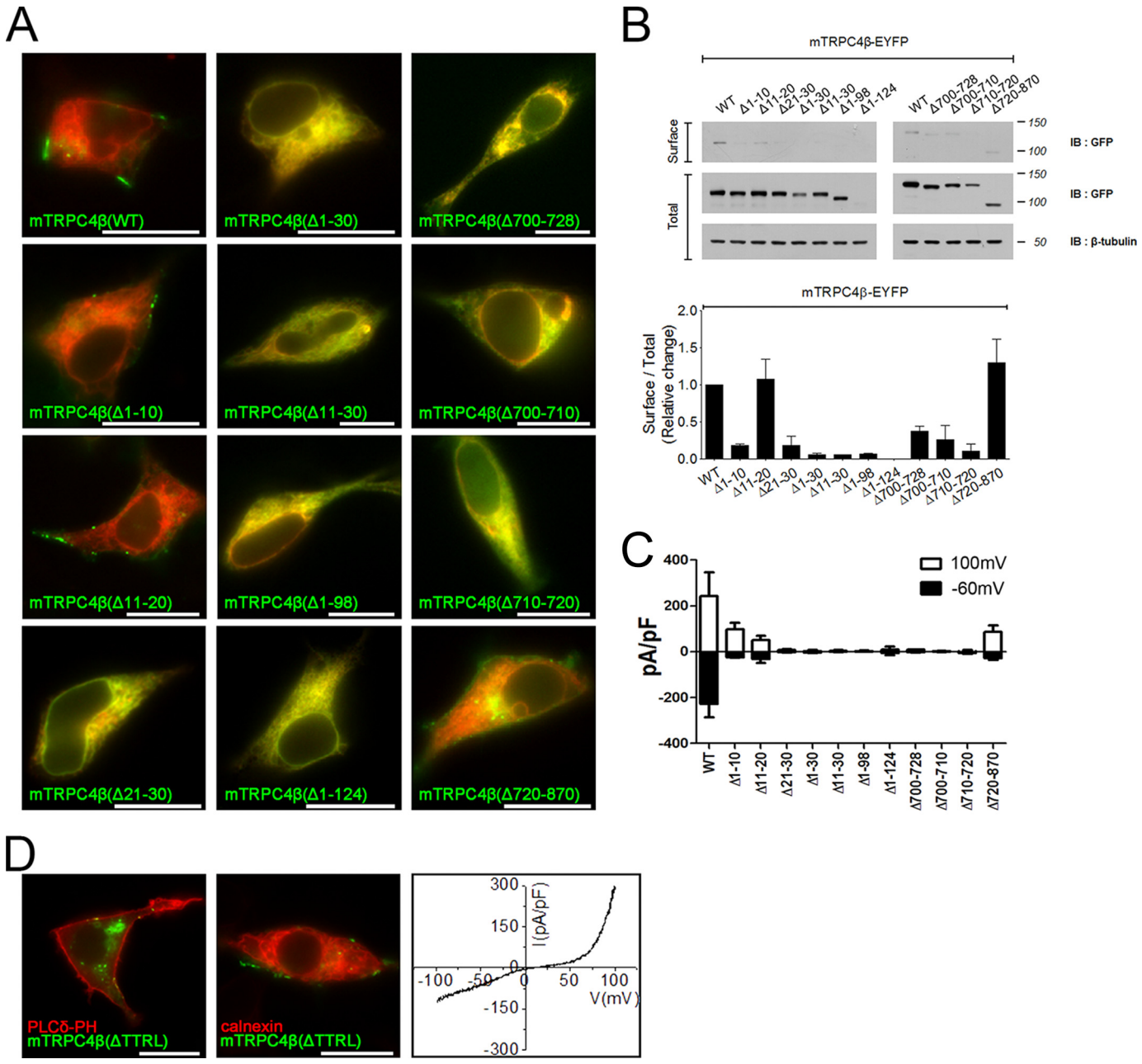

FIGURE 2. **Distribution, surface biotinylation, and whole cell current of deletion mutants of TRPC4.** *A*, CFP-tagged deletion mutants of TRPC4β (*green*) were coexpressed with calnexin-YPF (*red*), an ER resident chaperon, as an indicator of endoplasmic reticulum in HEK293 cells. TRPC4β-Δ21–30, TRPC4β-Δ 1–30, TRPC4β-Δ11–30, TRPC4β-Δ1–98, TRPC4β-Δ1–124, TRPC4β-Δ700–728, TRPC4β-Δ700–710, and TRPC4β-Δ710–720 deletion mutants were coexpressed with calnexin-YFP in endoplasmic reticulum. The scale bar represents 10 μm. *B*, Western blot of surface biotinylated YFP-tagged deletion mutants of TRPC4. Molecular mass in kDa is indicated on the *left*. *Lower panel*: the graph shows the quantification of surface biotinylation. Error bars indicate S.E. *C*, whole-cell patch clamp recordings reveal that cells that express TRPC4β (WT), TRPC4β (Δ1–10), TRPC4β (Δ11–20), and TRPC4β (Δ720–870) show robust GTPγ-induced currents (n = 3–10). The *white column* was measured with +100 mV, and the *black column* with −60 mV. Error bars indicate S.E. *D*, *left panel*: CFP-tagged TRPC4β with the deletion of the PDZ binding domain was coexpressed with PH-YFP as a marker of plasma membrane and with calnexin-YFP (*middle panel*) as a marker of endoplasmic reticulum. The scale bar represents 10 μm. *Right panel*: TRPC4β-ΔTTRL-CFP showed the double rectifying I/V shape in response to GTPγS (n = 4).

shows that the deleted regions are important for the insertion of the channels into the membrane. Consequently, when independently expressed, the Δ21–30, Δ1–30, Δ11–30, and Δ1–98 deletion mutants cannot be trafficked to the PM, but when co-expressed with WT, they are trafficked to the PM. Knowing that these mutants require the aid of WT to be trafficked to the PM, we can reasonably infer that the deleted regions of the deletion mutants, especially 21–30 aa, are the crucial regions for membrane insertion and punctate distribution at the PM. To confirm that TRPC4β (Δ21–30) could be expressed at the plasma membrane by forming tetrameric structures with TRPC4β-WT, we used surface biotinylation. To accomplish this goal, the cells were transfected with TRPC4β-Flag and TRPC4β-Δ21–30 or TRPC4β-Δ21–30 alone. A portion of the total lysate was retained to determine the expression levels of the transfected constructs. Biotinylated surface proteins

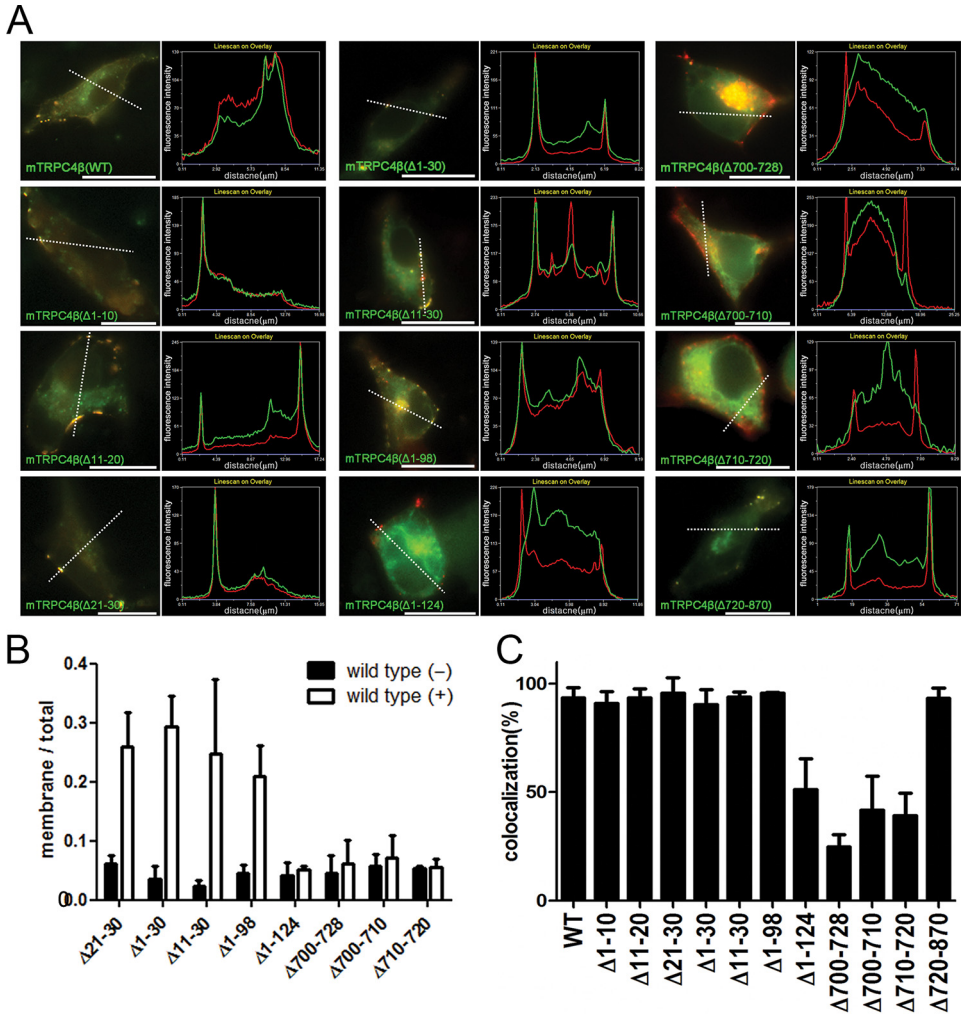

FIGURE 3. **Regulatory region of TRPC4 for membrane docking.** *A*, CFP-tagged deletion mutants of TRPC4β were coexpressed with TRPC4β (WT)-YFP in HEK293 cells. Cells that express TRPC4β (WT)-YFP and TRPC4β (WT, Δ1–10, Δ11–20, Δ21–30, Δ1–30, Δ11–30, Δ1–98, and Δ720–870)-CFP overlapped in the membrane, whereas other mutants were retained in the cytosol. The scale bar represents 10 μm. The line scan shows CFP-tagged mutants and mTRPC4β-WT-YFP intensity by the *white dashed line*. *B*, *black bar* indicates the fluorescence intensity ratio of the membrane expression of deletion mutants to whole cell expression when expressed alone. *White bar* indicates the fluorescence intensity ratio of deletion mutant expression when coexpressed with wild type. Error bars indicate S.E. *C*, overlapping regions of TRPC4β and deletion mutants of TRPC4β were measured at the plasma membrane. Error bars indicate S.E.

were then recovered by incubation with immobilized avidin-agarose. As shown in Fig. 4*A*, although the cell total fraction of the band for the TRPC4β-Δ21–30 that co-expressed with TRPC4β-WT-Flag appeared to be less dense than that derived from cells transfected with TRPC4β-Δ21–30 alone, we found that the level of TRPC4β-Δ21–30 co-expressed with TRPC4β-WT-Flag increased in the cell surface compared with TRPC4β-Δ21–30 alone. A similar result was obtained for TRPC4β-Δ11–30 (Fig. 4*A*). However, TRPC4β-WT did not increase the expression of TRPC4β-Δ1–124 at the cell surface. Nevertheless, all of the cotransfected cells showed the typical TRPC4 current with a double rectifying shape (Fig. 4*B*).

As observed in the TRPC4 channel, when TRPC5- Δ21–30 is expressed in the HEK293 cell, the mutants were retained in the endoplasmic reticulum (Fig. 4*C*). However, when TRPC5-Δ21–30 is co-expressed with TRPC5-WT with the aid of the wild type, TRPC5-Δ21–30 is successfully expressed in the membrane (Fig. 4*D*). These results suggest that the 21–30 domain of the TRPC5 and TRPC4 channels was responsible for the membrane trafficking and punctate distribution but not for channel tetramerization.

Amino Acids 23–29 of the TRPC4 Channel Is the Critical Region for Membrane Insertion—To investigate whether the ER retention due to the deletion of the 21–30 aa of TRPC4 is the result of the deletion and consequent conformational change of the channel, we inserted the 21–30 aa region of TRPC1 into the relevant region of TRPC4, which is in the same group as TRPC1 (Fig. 5*A*). hTRPC1 alpha and beta are retained in the endoplasmic reticulum (Fig. 5*B*) and could make a hetero tetrameric structure with TRPC4 and TRPC5 (27). Thus, we generated chimera mutants of fluorescence-tagged TRPC4β by changing TRPC4β 23–29 aa with the corresponding TRPC1α aa; specifically, TRPC4β (23–29, C1), TRPC4β (25–29, C1), TRPC4β (23–29, C1) and TRPC4β (23–26, C1). TRPC4β (27–29, C1), TRPC4β (25–29, C1), and TRPC4β (23–26, C1) were expressed at the PM, whereas TRPC4β (23–29, C1) were expressed in the intracellular compartments (Fig. 6*A*). By co-localization studies, ER retention for TRPC4β (23–29, C1) was confirmed.

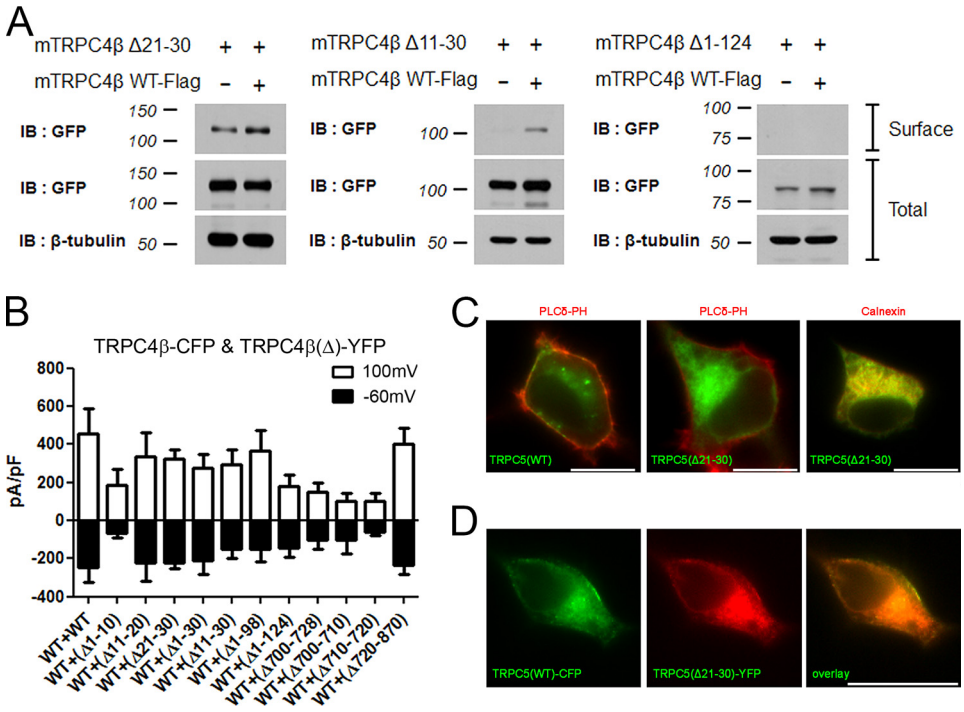

FIGURE 4. **Coexpression of deletion mutants and wild type channel.** Distribution of TRPC5- Δ21–30 amino acids. *A*, for Western blot of surface biotinylation, *left column*: TRPC4β (Δ21–30)- CFP was transfected alone and cotransfected with TRPC4β (WT)-Flag in HEK293 cells. Reduced expression of TRPC4β (Δ21–30)-CFP was detected in the membrane compared with coexpression with TRPC4β (WT)-Flag. *Middle column*: for Western blot of surface biotinylation, TRPC4β-Δ11–30-CFP was transfected alone and cotransfected with TRPC4β-WT-Flag in HEK293 cells. *Right panel* shows Western blot of surface biotinylation of TRPC4β-Δ1–124-CFP when expressed alone or coexpressed with wild type. The molecular mass in kDa is indicated on the *left*. *Lower panel*: the anti-actin antibody was used as a loading control. *B*, whole-cell patch clamp recordings of all of the cells coexpressing TRPC4β-WT and deletion mutants showed robust GTPγ-induced currents ($n = 3–8$). The *white column* was measured with +100 mV, and the *black column* with −0 mV. Error bars indicate S.E. *C*, *left*: wild-type CFP-TRPC5 (*green*) showed a punctate distribution in the plasma membrane. PH-YFP (*red*) is an indicator of the plasma membrane. *Middle*: 21–30 aa deleted mutant of TRPC5 was coexpressed with PH-YFP (*red*) and calnexin-YFP (*red*, *right*). The scale bar represents 10 μm. *D*, coexpression of CFP-TRP5 (*green*, *left*) and YFP- TRPC5 (Δ21–30) (*red*, *middle*) showed colocalization in the membrane (*right*). The scale bar represents 10 μm.

TRPC4β (23–29, C1) overlaps with the ER resident chaperone calnexin. Co-localization of TRPC4β (23–29, C1) with the Golgi marker, FAPP1, was not detected. TRPC4 chimera were trafficked when 27–29, 25–29, or 23–26 aa of the TRPC4β channel were substituted with the relevant part of TRPC1, whereas independently expressed TRPC4β (23–29, C1) could not be located at the PM. When the chimera mutants co-expressed with WT, however, all four chimera were successfully located at the PM (Fig. 6*B*). The function of the chimera mutants was tested with a patch clamp technique (Fig. 6*C*). Except for TRPC4β (23–29, C1) chimera, other chimera mutants showed I/V curves that had the general TRPC4 double rectifying shape in response to GTPγS. These findings, up to this point, demonstrate that N terminus 23–29 aa of TRPC4 is a critical region for insertion into the PM.

Additionally, we confirmed TRPC4β-Δ23–24, TRPC4β-Δ31–40, TRPC4β-Δ41–50, TRPC4β-Δ1–68, and TRPC4β-Δ1–170 mutants were also retained in the ER (data not shown). By a chimera mutants experiment, we more focused on 21–30 region rather than downstream of 30th aa. However, it is possible that downstream of the 30th aa influence trafficking.

The Important Region for the Formation of the TRPC4 Tetrameric Structure—Collecting these data, we hypothesized that deletion mutants that impaired proper folding and could not insert into the PM were not expressed alone and were not coexpressed with the wild type TRPC4. Fig. 3*A* showed that TRPC4β-Δ1–124, TRPC4β-Δ700–728, TRPC4β-Δ700–710, and TRPC4β-Δ710–720 failed to reach the plasma membrane and showed ER retention even if co-expressed with TRPC4β-WT. In other words, the preceding 4 deletion mutants were not properly folded or assembled with the wild type. From these results, we assumed that there are two regions that are responsible for the tetrameric assembly of TRPC4 channels. First, the N terminus region from the 98th aa to the 124th aa is one of the regions for making a tetrameric structure. The reason is that the mutants that were deleted further than the 98th aa could not be trafficked into the PM even with the aid of TRPC4-WT. Second, the deleted SESTD1 and CIRB domain showed the same phenomenon by deletion. For the C terminus deletion mutants TRPC4β-Δ700–728, TRPC4β-Δ700–710, and TRPC4β-Δ710–720, the channels could not be trafficked to the PM as well as when co-expressed with WT (9–11). The SESTD1 (SEC14-like and spectrin-type domain 1) binding domain of TRPC4 and TRPC5 is crucial for proper working and regulation (5, 28). This sequence is highly conserved in TRPC5 and largely overlaps with the CIRB domain.

To demonstrate the tetrameric structure conformation and ion channel function of pore-forming mutants and to find the self-assembly domain in living cells, we used the 3-cube FRET technique (18). We co-expressed CFP- or YFP-tagged wild type TRPC4 and CFP- or YFP-tagged deletion mutants of the TRPC4 channel. As a negative control experiment, the FRET efficiency between TRPC4-CFP and empty-YFP was measured

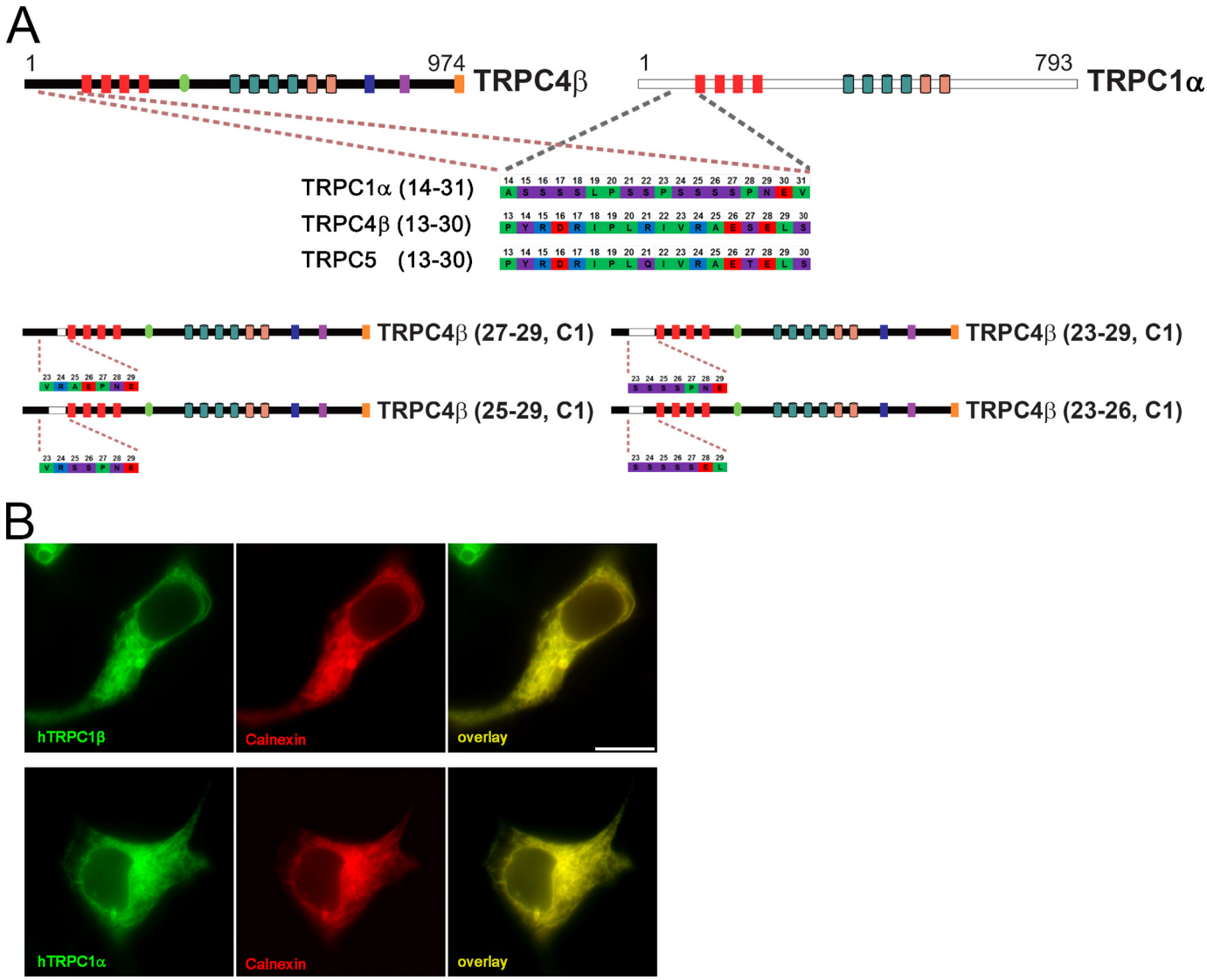

FIGURE 5. **Chimera mutants of TRPC4 and expression of hTRPC1.** *A*, diagram of TRPC4, TRPC1, and chimera mutants of TRPC4. Four chimera mutants were made by fragments of TRPC1 insertions into the backbone of TRPC4β. *B*, CFP-tagged hTRPC1β (*upper*) and hTRPC1α (*lower*) were coexpressed with calnexin-YFP as an indicator of ER. The scale bar represents 10 μm.

and was less than 1%. As a positive control experiment, the FRET efficiency between TRPC4β-WT-CFP and TRPC4β-WT-YFP at the plasma membrane was measured and was robust (22.25 ± 0.76%, $n = 73$). The FRET signal between TRPC4-WT-CFP and the deletion mutants that were trafficked to the membrane when co-expressed with TRPC4β-WT (TRPC4β-Δ1–10-YFP (19.28 ± 2.50%, $n = 5$), TRPC4β-Δ11–20-YFP (24.14 ± 2.25%, $n = 4$), TRPC4β-Δ21–30-YFP (21.62 ± 1.91%, $n = 4$), TRPC4β-Δ1–30-YFP (22.26 ± 3.06%, $n = 7$), and TRPC4β-Δ1–98-YFP (19.47 ± 2.60%, $n = 5$)) were similar to the FRET signal between TRPC4β-WT-CFP and TRPC4β-WT-YFP FRET (Fig. 7*A*). These FRET signals between the WT and mutants could be trafficked only with the aid of WT, which suggests that these mutants can form heterotetrameric structures in the WT. At the plasma membrane, however, the FRET signal of mTRPC4β-WT-CFP with mTRPC4β-Δ1–124-YFP (3.00 ± 1.52%, $n = 8$) and mTRPC4β-Δ700–728-YFP (1.13 ± 0.40%, $n = 8$), which could not be trafficked to the PM, were lower even than with mTRPC4β-WT in the plasma membrane. Interestingly, the FRET signal between TRPC4β-WT-CFP and TRPC4β-Δ720–870-YFP (14.32 ± 1.32%, $n = 5$) was lower than the positive control. This finding of reduced FRET efficiency appears to be due to the loss of the 150 aa in the C terminus of TRPC4β. Consequently, CFP and YFP were separated further compared with the C terminus-tagged fluorescence proteins and TRPC4β-WT.

In cytosol, the FRET efficiency was detected between all of the deletion mutants and TRPC4β-WT-CFP (Fig. 7*B*). The FRET efficiency between the deletion mutants that could make the tetrameric structure in the plasma membrane (TRPC4β-Δ1–10-YFP (16.06 ± 2.04%, $n = 9$), TRPC4β-Δ11–20-YFP (15.53 ± 2.68%, $n = 7$), TRPC4β-Δ21–30-YFP (15.10 ± 1.87%, $n = 9$), TRPC4β-Δ1–30-YFP (15.60 ± 1.79%, $n = 6$), and TRPC4β-Δ1–98-YFP (19.47 ± 2.60%, $n = 5$)) and TRPC4β-WT-CFP were similar to the FRET efficiency with TRPC4β-WT-YFP (18.93 ± 2.08%, $n = 11$). Unexpectedly, mTRPC4β-Δ1–124-YFP (8.68 ± 1.40%, $n = 13$) and mTRPC4β-Δ700–728-YFP (10.40 ± 1.39%, $n = 7$)

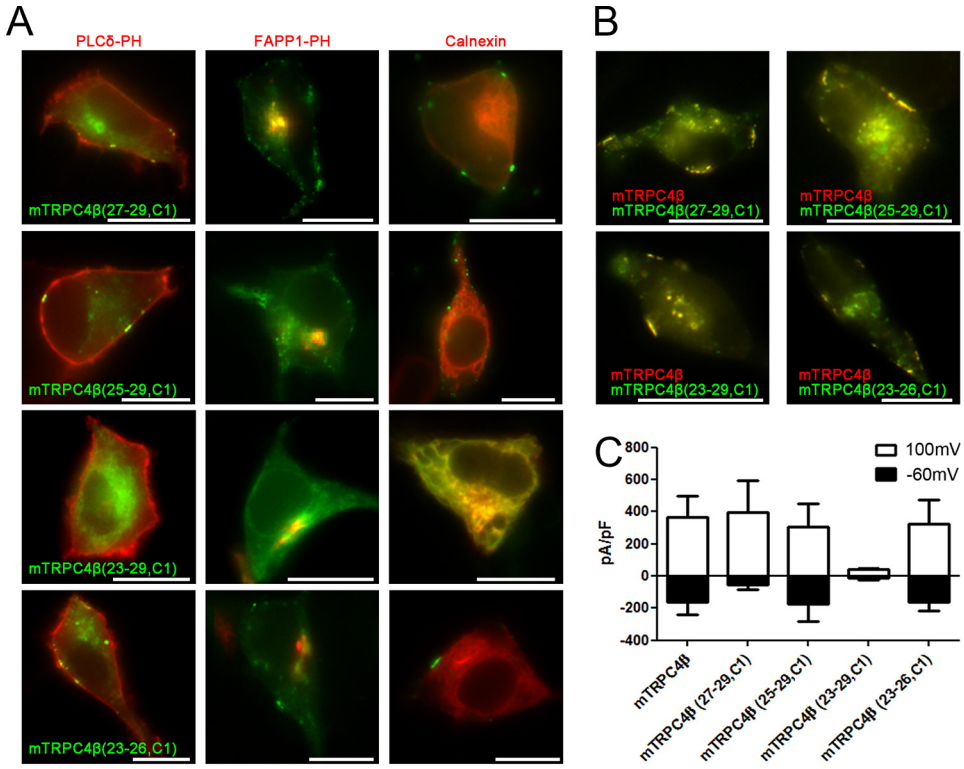

FIGURE 6. **23–29 of the TRPC4 channel is the critical region for membrane insertion.** *A*, *left column*: CFP-tagged chimera mutants, TRPC4β (27–29, C1), TRPC4β (25–29, C1), TRPC4β (23–29, C1), and TRPC4β (23–26, C1), were cotransfected with YFP-tagged PLCδ-PH in HEK293 cells. *Middle column*: CFP-tagged chimera mutants were coexpressed with YFP-tagged FAPP1-PH, to be a Golgi marker. *Right column*: CFP-tagged chimera mutants were coexpressed with YFP-tagged calnexin, to be an ER marker. Chimera mutants expressed a punctate distribution in the membrane except for TRPC4β (23–29, C1). The scale bar represents 10 μm. *B*, chimera mutants (*green*) were expressed with the wild type TRPC4β (*red*). All of the chimera mutants expressed in the plasma membrane involved TRPC4β (23–29, C1), which was expressed in the ER when transfected alone. The scale bar represents 10 μm. *C*, whole-cell patch clamp recordings reveal that cells that expressed chimera mutants show robust GTPγ-induced currents, except for mTRPC4β (23–29, C1) (n = 3–10). The *white column* was measured with +100 mV, and the *black column* with −60 mV. Error bars indicate S.E.

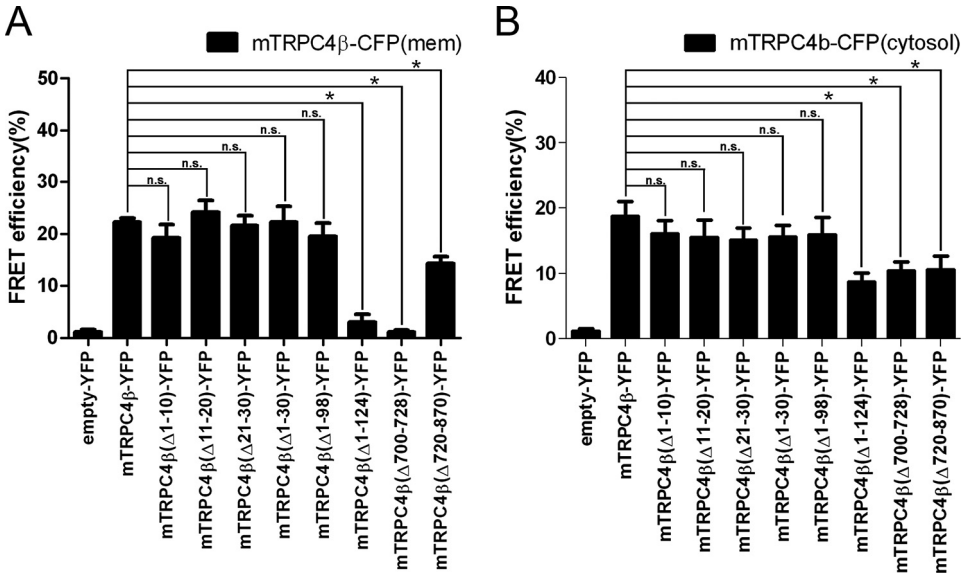

FIGURE 7. **The important region for the formation of the TRPC4 tetrameric structure.** *A*, in the plasma membrane and *B*, cytosol, the FRET efficiency between YFP-tagged deletion mutants of the TRPC4β channel and CFP-tagged TRPC4β (WT) channel was quantified by 3-cube FRET. FRET between empty-YFP and TRPC4β (WT)-CFP was a control experiment. Error bars indicate S.E. Here, *, $p < 0.05$ was statistically significant. *n.s.*, not significant.

have significantly reduced the FRET efficiency but have greater FRET efficiency than that at the PM. TRPC4β-Δ720–870-YFP (14.32 ± 1.32%, n = 5) has a similar FRET efficiency to that at the PM.

Candidates for Regulators of TRPC4 Channel Trafficking—We investigated which candidate molecules interact with the 23–29 aa of the TRPC4 channel and, consequently, regulate the channel trafficking and punctate distribution at the PM. Previ-

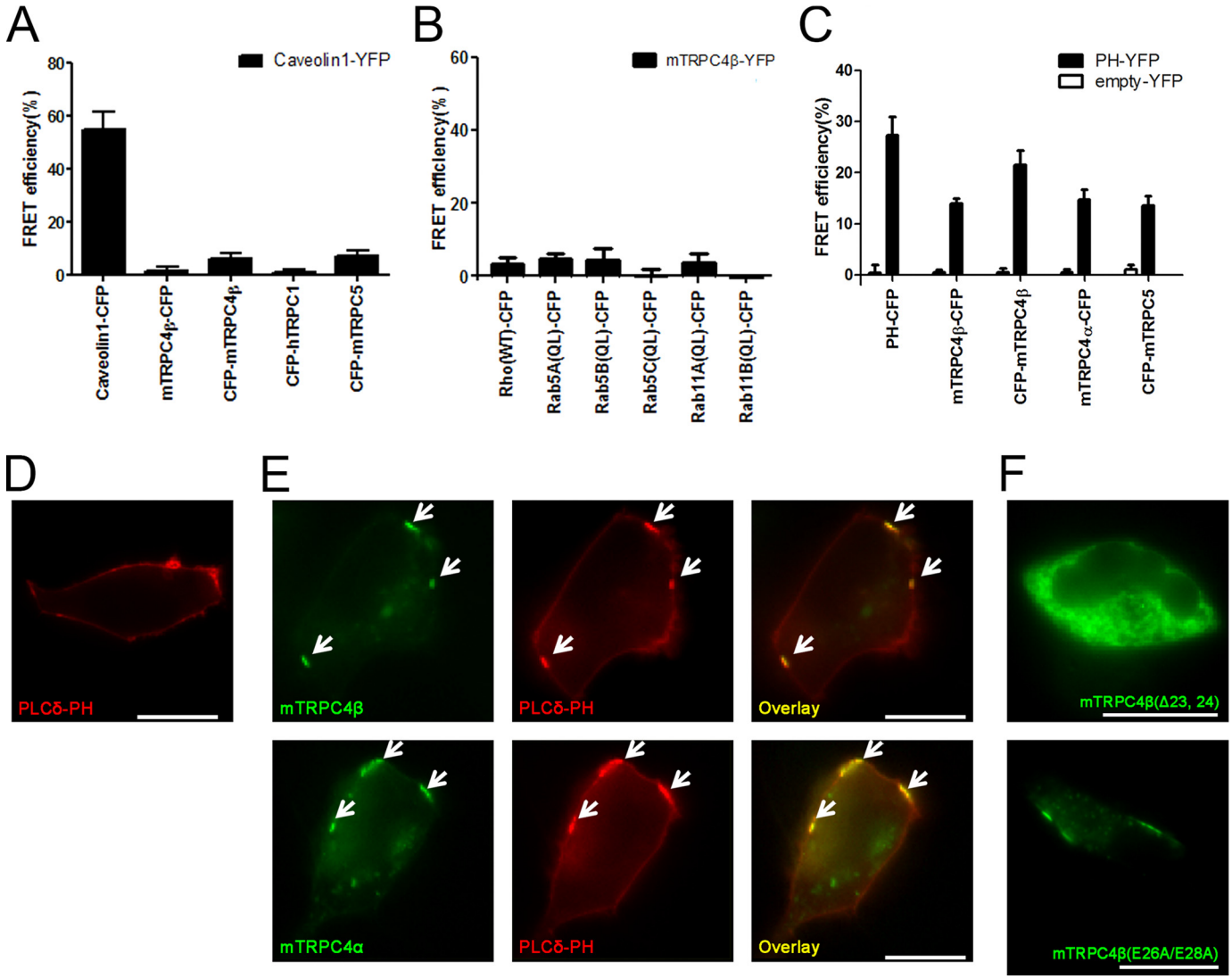

FIGURE 8. **Candidates for the regulator of TRPC4 channel trafficking and distribution of mTRPC4β-Δ23,24 and mTRPC4β-E26A/E28A.** *A*, FRET efficiency between caveolin-YFP and CFP-tagged TRPC channels. FRET between caveolin-CFP and caveolin-YFP was a control experiment. *B*, FRET efficiency between TRPC4β-YFP and small G proteins. FRET between empty-CFP and TRPC4β-YFP was a control experiment. *C*, FRET efficiency between PH-YFP (*black bar*), and empty- YFP (*white bar*) and CFP-tagged TRPC4α, β and TRPC5. Error bars indicate S.E. *D*, PH-YFP was transfected in HEK293 cells. *E*, *upper panel*: TRPC4β-CFP and PH-YFP were expressed in HEK293 cells. *Lower panel*: TRPC4β-CFP and PH-YFP were expressed in HEK293 cells. *F*, mTRPC4β-Δ23, 24-CFP and mTRPC4β-E26A/E28A-CFP show *green* in the image. The scale bar represents 10 μm.

ous studies have shown that the following candidates, for example, caveolin (29), $PI(4,5)P_2$ (30), small G protein (31), cytoskeleton, SESTD1 (28), and protein 4.1 (32), interacted with TRPC4 and could regulate membrane trafficking and docking.

Initially, caveolin making caveolae and lipid raft multi-structure was known to be a regulator of membrane expression of the TRP channel (33–35). Especially caveolin knock-out mouse showed ER retention of the TRPC4 channel (36). Caveolin is well known as a molecule that is associated with caveolae and regulates their formation by multimeric structure. The caveolin binding site (CBS) of caveolin-interacting proteins, for example, the eNOS, PKC, MEK, ERK, Ras, G protein, and EGF receptor, interacts with the caveolin scaffolding domain (CSD), which is 82–101 aa of caveolin (37). Usually, CBS has a typical pattern, such as $\Phi X\Phi XXXX\Phi$, $\Phi XXXX\Phi XX\Phi$ or $\Phi X\Phi XXXX\Phi XX\Phi$, where Φ is an aromatic amino acid. The 21–50 aa of the TRPC4 channel do not match with CBS. In addition, the FRET efficiency between caveolin 1-YFP with mTRPC4β-CFP (1.36 ± 1.47%, $n = 4$), CFP-mTRPC4β (4.78 ± 2.06%, $n = 5$), CFP-hTRPC1 (0.23 ± 1.30%, $n = 4$) and CFP-mTRPC5 (0.23 ± 1.30%, $n = 4$) were lower than 5%, whereas robust FRET efficiency was detected between caveolin 1-CFP and caveolin 1-YFP (54.87 ± 6.46%, $n = 4$) (Fig. 8*A*).

Second, the FRET efficiency between TRPC4 with the small G protein, Rho (3.18 ± 2.02%, $n = 4$), Rab5A (4.91 ± 1.30%, $n = 4$), Rab5B (4.35 ± 3.33%, $n = 3$), Rab5C (0.05 ± 1.71%, $n = 4$), Rab11A (3.83 ± 2.52%, $n = 3$), and Rab11B (0.53 ± 1.89%, $n = 3$), was lower than 5% (Fig. 8*B*). Protein 4.1 (32), VAMP (38), phosphorylation (39), spectrin (8), and cAMP (40) are known to regulate the expression of the TRPC4 channel at the PM, but their interaction with the N terminus of the TRPC4 channel has been unknown.

Third, $PI(4,5)P_2$ is the other candidate for the trafficking of TRPC4. $PI(4,5)P_2$ has been known to regulate the gating of

GIRK channel, and GIRK's x-ray crystal structure showed that four $PI(4,5)P_2$ interact with each GIRK, making a tetrameric structure of the channel (41). $PI(4,5)P_2$ exists as almost 1% of the plasma lipids and is rich in caveola. The interaction of the TRPC4 channel with $PI(4,5)P_2$ was well known (30, 42). It is reported that the N terminus of other TRP channels interacts with $PI(4,5)P_2$ (43–46). As a positive control experiment, the FRET efficiency between PH-YFP and PH-CFP was 27.27 ± 3.59% ($n = 5$). The FRET efficiency between PH-YFP and mTRPC4β (WT)-CFP was 13.87 ± 0.99% ($n = 5$); CFP-mTRPC4β, 21.49 ± 2.82% ($n = 8$); mTRPC4α-CFP, 14.68 ± 2.01% ($n = 8$); and CFP-mTRPC5, 13.55 ± 1.80% ($n = 9$) (Fig. 8*C*). YFP tagged at the N terminus of the TRPC4 channel showed the highest FRET efficiency with CFP-PH. Interestingly, when HEK293 cells were transfected with the CFP- or YFP-tagged PH domain of PLCδ, these proteins were expressed uniformly at the plasma membrane (Fig. 8*D*). However, when HEK cells were co-transfected with PH-YFP and CFP-tagged TRPC4 alpha or beta, PH-YFP showed a punctate distribution following the punctate expression of the TRPC4 channel (Fig. 8*E*). This result does not match with the report that shows that an alternatively spliced domain of TRPC4β (84 aa from 781–864) binds with $PI(4,5)P_2$ (42). These results suggest that $PI(4,5)P_2$ might interact with 23–29 aa at the N terminus of TRPC4 to regulate the membrane expression. The depletion of $PI(4,5)P_2$ by the rapamycin-inducible system irreversibly inhibited the TRPC4 current (30). In turn, the depletion of $PI(4,5)P_2$ might induce endocytosis of the TRPC4 channel from the PM.

Finally, the Val^{57}-Thr^{58}-Val^{59} tripeptide at the N terminus of human concentrative nucleoside transporter 3 (hCNT3) appears to be the core of the endoplasmic reticulum export signal (47). Our preceding results have demonstrated that the ^{23}VRAETEL^{29} aa residues require TRPC4 expression at the cell surface. This domain of TRPC4 and TRPC5 also contains ^{26}EXE^{28}, which is very similar to the di-acidic ER export motifs that have been identified in several plasma membrane proteins (48–52). However, TRPC4β (E26A/E28A) but not the (Δ23, 24) channel were expressed at the plasma membrane (Fig. 8*F*).

DISCUSSION

The present studies showed that 1) N terminus 23–29 aa of TRPC4 are a crucial domain for membrane insertion of channel proteins, 2) modifying this domain could cause trafficking to the plasma membrane by making proper folding or heterotetrameric assembly with wild type TRPC4, 3) N or C terminus interact with each other to make a tetrameric structure, 4) $PI(4,5)P_2$ is a possible candidate for interaction with the membrane-targeting domain at the N terminus of TRPC4, and 5) N terminus 98–124 aa and C terminus 700–728 aa are critical for the tetrameric assembly of TRPC4.

By the imaging approach, we could find a membrane-targeting domain of the channels independent of the domains that are critical for the tetrameric or dimeric structure. The ^{23}VRAETEL^{29} aa residues are required for TRPC4 expression at the cell surface (Fig. 6). This domain is not related to ER export. The N terminus of the TRPC3 channel acts as a half-domain of the PH domain with the PLCγ PH domain (45, 53–55). The report also showed that the TRPC4 N terminus has a similar amino acid sequence and acts as a half domain of the PH domain.

There was a correlation between the whole cell current and the punctate distribution at the PM of the TRPC4 channel (Figs. 1 and 2) and between trafficking into the plasma membrane (surface biotinylation) and the punctate distribution at the PM of the TRPC4 channel, except for TRPC4-Δ1–10 (Fig. 2). This exception might occur due to the specific definition of PM expression. We defined PM expression of the TRPC4 channel to occur when the TRPC4 channel distributes as a patch or puncta rather than a random distribution at the PM. In the case of the TRP channels, to distinguish the subplasmalemmal distribution from the PM distribution was difficult. The TRPC4-Δ1–10 deletion mutant might localize uniquely at a specific area and function in a more efficient way even though the total protein at the cell surface is lower. A similar result was obtained in TRPV5 (24).

The patch clamp technique is useful for measuring the current from the functioning ion channels. In our hands, this technique has been very sensitive and reliable for the TRPC4 channels (5, 14–16, 22, 30). On the other hand, this technique was not good for the rescue experiment of deletion mutants with TRPC4-WT or the co-expression experiment of more than 2 constructs (Figs. 2*C* and 4*B*). In general, making a dimer or tetramer construct takes a long time, and dimer or tetramer constructs usually do not work well due to the linker length or the flexibility of the linker (22). To combine the imaging methods and the FRET methods was useful for finding a membrane-targeting domain or tetrameric assembly domain.

In the present study, we found a novel membrane-targeting sequence (^{23}VRAETEL^{29}) of TRPC4 channels. The N terminus region (98–124 aa) and the C terminus region (700–728 aa) are critical for tetrameric assembly.

REFERENCES

1. Xu, X. Z., Moebius, F., Gill, D. L., and Montell, C. (2001) Regulation of melastatin, a TRP-related protein, through interaction with a cytoplasmic isoform. *Proc. Natl. Acad. Sci. U. S. A.* **98,** 10692–10697
2. van de Graaf, S. F., Hoenderop, J. G., Gkika, D., Lamers, D., Prenen, J., Rescher, U., Gerke, V., Staub, O., Nilius, B., and Bindels, R. J. (2003) Functional expression of the epithelial Ca(2+) channels (TRPV5 and TRPV6) requires association of the S100A10-annexin 2 complex. *EMBO J.* **22,** 1478–1487
3. Wedel, B. J., Vazquez, G., McKay, R. R., St, J. Bird, G., and Putney, J. W., Jr. (2003) A calmodulin/inositol 1,4,5-trisphosphate (IP3) receptor-binding region targets TRPC3 to the plasma membrane in a calmodulin/IP3 receptor-independent process. *J. Biol. Chem.* **278,** 25758–25765
4. Andrade, Y. N., Fernandes, J., Vázquez, E., Fernández-Fernández, J. M., Arniges, M., Sánchez, T. M., Villalón, M., and Valverde, M. A. (2005) TRPV4 channel is involved in the coupling of fluid viscosity changes to epithelial ciliary activity. *J. Cell Biol.* **168,** 869–874
5. Jeon, J. P., Hong, C., Park, E. J., Jeon, J. H., Cho, N. H., Kim, I. G., Choe, H., Muallem, S., Kim, H. J., and So, I. (2012) Selective Gαi subunits as novel direct activators of transient receptor potential canonical (TRPC)4 and TRPC5 channels. *J. Biol. Chem.* **287,** 17029–17039
6. Ordaz, B., Tang, J., Xiao, R., Salgado, A., Sampieri, A., Zhu, M. X., and Vaca, L. (2005) Calmodulin and calcium interplay in the modulation of TRPC5 channel activity. Identification of a novel C-terminal domain for calcium/calmodulin-mediated facilitation. *J. Biol. Chem.* **280,** 30788–30796
7. Mery, L., Strauss, B., Dufour, J. F., Krause, K. H., and Hoth, M. (2002) The PDZ-interacting domain of TRPC4 controls its localization and surface expression in HEK293 cells. *J. Cell Sci.* **115,** 3497–3508

8. Odell, A. F., Van Helden, D. F., and Scott, J. L. (2008) The spectrin cytoskeleton influences the surface expression and activation of human transient receptor potential channel 4 channels. *J. Biol. Chem.* **283,** 4395–4407
9. Schindl, R., Frischauf, I., Kahr, H., Fritsch, R., Krenn, M., Derndl, A., Vales, E., Muik, M., Derler, I., Groschner, K., and Romanin, C. (2008) The first ankyrin-like repeat is the minimum indispensable key structure for functional assembly of homo- and heteromeric TRPC4/TRPC5 channels. *Cell Calcium* **43,** 260–269
10. Lepage, P. K., Lussier, M. P., McDuff, F. O., Lavigne, P., and Boulay, G. (2009) The self-association of two N-terminal interaction domains plays an important role in the tetramerization of TRPC4. *Cell Calcium* **45,** 251–259
11. Lepage, P. K., Lussier, M. P., Barajas-Martinez, H., Bousquet, S. M., Blanchard, A. P., Francoeur, N., Dumaine, R., and Boulay, G. (2006) Identification of two domains involved in the assembly of transient receptor potential canonical channels. *J. Biol. Chem.* **281,** 30356–30364
12. Liao, M., Cao, E., Julius, D., and Cheng, Y. (2013) Structure of the TRPV1 ion channel determined by electron cryo-microscopy. *Nature* **504,** 107–112
13. Kim, H., Kim, J., Jeon, J. P., Myeong, J., Wie, J., Hong, C., Kim, H. J., Jeon, J. H., and So, I. (2012) The roles of G proteins in the activation of TRPC4 and TRPC5 transient receptor potential channels. *Channels* **6,** 333–343
14. Kim, M. T., Kim, B. J., Lee, J. H., Kwon, S. C., Yeon, D. S., Yang, D. K., So, I., and Kim, K. W. (2006) Involvement of calmodulin and myosin light chain kinase in activation of mTRPC5 expressed in HEK cells. *Am. J. Physiol.* **290,** C1031–C1040
15. So, I., and Kim, K. W. (2003) Nonselective cation channels activated by the stimulation of muscarinic receptors in mammalian gastric smooth muscle. *J. Smooth Muscle Res.* **39,** 231–247
16. Kim, M. J., Jeon, J. P., Kim, H. J., Kim, B. J., Lee, Y. M., Choe, H., Jeon, J. H., Kim, S. J., and So, I. (2008) Molecular determinant of sensing extracellular pH in classical transient receptor potential channel 5. *Biochem. Biophys. Res. Commun.* **365,** 239–245
17. Yan, H. D., Okamoto, H., Unno, T., Tsytsyura, Y. D., Prestwich, S. A., Komori, S., Zholos, A. V., and Bolton, T. B. (2003) Effects of G-protein-specific antibodies and G$\beta\gamma$ subunits on the muscarinic receptor-operated cation current in guinea-pig ileal smooth muscle cells. *Br. J. Pharmacol.* **139,** 605–615
18. Erickson, M. G., Alseikhan, B. A., Peterson, B. Z., and Yue, D. T. (2001) Preassociation of calmodulin with voltage-gated Ca(2+) channels revealed by FRET in single living cells. *Neuron* **31,** 973–985
19. Patterson, G., Day, R. N., and Piston, D. (2001) Fluorescent protein spectra. *J. Cell Sci.* **114,** 837–838
20. Miyawaki, A., and Tsien, R. Y. (2000) Monitoring protein conformations and interactions by fluorescence resonance energy transfer between mutants of green fluorescent protein. *Methods Enzymol.* **327,** 472–500
21. Epe, B., Steinhäuser, K. G., and Woolley, P. (1983) Theory of measurement of Forster-type energy transfer in macromolecules. *Proc. Natl. Acad. Sci. U. S. A.* **80,** 2579–2583
22. Hong, C., Kwak, M., Myeong, J., Ha, K., Wie, J., Jeon, J. H., and So, I. (2014) Extracellular disulfide bridges stabilize TRPC5 dimerization, trafficking, and activity. *Pflugers Archiv*
23. Amiri, H., Schultz, G., and Schaefer, M. (2003) FRET-based analysis of TRPC subunit stoichiometry. *Cell Calcium* **33,** 463–470
24. de Groot, T., van der Hagen, E. A., Verkaart, S., te Boekhorst, V. A., Bindels, R. J., and Hoenderop, J. G. (2011) Role of the transient receptor potential vanilloid 5 (TRPV5) protein N terminus in channel activity, tetramerization, and trafficking. *J. Biol. Chem.* **286,** 32132–32139
25. Song, X., Zhao, Y., Narcisse, L., Duffy, H., Kress, Y., Lee, S., and Brosnan, C. F. (2005) Canonical transient receptor potential channel 4 (TRPC4) co-localizes with the scaffolding protein ZO-1 in human fetal astrocytes in culture. *Glia* **49,** 418–429
26. Raucher, D., Stauffer, T., Chen, W., Shen, K., Guo, S., York, J. D., Sheetz, M. P., and Meyer, T. (2000) Phosphatidylinositol 4,5-bisphosphate functions as a second messenger that regulates cytoskeleton-plasma membrane adhesion. *Cell* **100,** 221–228
27. Hofmann, T., Schaefer, M., Schultz, G., and Gudermann, T. (2002) Subunit composition of mammalian transient receptor potential channels in living cells. *Proc. Natl. Acad. Sci. U. S. A.* **99,** 7461–7466
28. Miehe, S., Bieberstein, A., Arnould, I., Ihdene, O., Rütten, H., and Strübing, C. (2010) The phospholipid-binding protein SESTD1 is a novel regulator of the transient receptor potential channels TRPC4 and TRPC5. *J. Biol. Chem.* **285,** 12426–12434
29. Murakami, M., Ohba, T., Xu, F., Shida, S., Satoh, E., Ono, K., Miyoshi, I., Watanabe, H., Ito, H., and Iijima, T. (2005) Genomic organization and functional analysis of murine PKD2L1. *J. Biol. Chem.* **280,** 5626–5635
30. Kim, H., Jeon, J. P., Hong, C., Kim, J., Myeong, J., Jeon, J. H., and So, I. (2013) An essential role of PI(4,5)P(2) for maintaining the activity of the transient receptor potential canonical (TRPC)4β. *Pflugers Archiv* **465,** 1011–1021
31. Cayouette, S., and Boulay, G. (2007) Intracellular trafficking of TRP channels. *Cell Calcium* **42,** 225–232
32. Cioffi, D. L., Wu, S., Alexeyev, M., Goodman, S. R., Zhu, M. X., and Stevens, T. (2005) Activation of the endothelial store-operated ISOC Ca2+ channel requires interaction of protein 4.1 with TRPC4. *Circulation Research* **97,** 1164–1172
33. Gervásio, O. L., Whitehead, N. P., Yeung, E. W., Phillips, W. D., and Allen, D. G. (2008) TRPC1 binds to caveolin-3 and is regulated by Src kinase - role in Duchenne muscular dystrophy. *J. Cell Sci.* **121,** 2246–2255
34. Brazer, S. C., Singh, B. B., Liu, X., Swaim, W., and Ambudkar, I. S. (2003) Caveolin-1 contributes to assembly of store-operated Ca2+ influx channels by regulating plasma membrane localization of TRPC1. *J. Biol. Chem.* **278,** 27208–27215
35. Brownlow, S. L., and Sage, S. O. (2005) Transient receptor potential protein subunit assembly and membrane distribution in human platelets. *Thrombosis Haemostasis* **94,** 839–845
36. Murata, T., Lin, M. I., Stan, R. V., Bauer, P. M., Yu, J., and Sessa, W. C. (2007) Genetic evidence supporting caveolae microdomain regulation of calcium entry in endothelial cells. *J. Biol. Chem.* **282,** 16631–16643
37. Tourkina, E., and Hoffman, S. (2012) Caveolin-1 signaling in lung fibrosis. *Open Rheumatol. J.* **6,** 116–122
38. Montell, C. (2005) The TRP superfamily of cation channels. *Science's STKE : signal transduction knowledge environment* 2005, re3
39. Odell, A. F., Scott, J. L., and Van Helden, D. F. (2005) Epidermal growth factor induces tyrosine phosphorylation, membrane insertion, and activation of transient receptor potential channel 4. *J. Biol. Chem.* **280,** 37974–37987
40. Zhang, S., Remillard, C. V., Fantozzi, I., and Yuan, J. X. (2004) ATP-induced mitogenesis is mediated by cyclic AMP response element-binding protein-enhanced TRPC4 expression and activity in human pulmonary artery smooth muscle cells. *Am. J. Physiol.* **287,** C1192–C1201
41. Whorton, M. R., and MacKinnon, R. (2013) X-ray structure of the mammalian GIRK2-$\beta\gamma$ G-protein complex. *Nature* **498,** 190–197
42. Otsuguro, K., Tang, J., Tang, Y., Xiao, R., Freichel, M., Tsvilovskyy, V., Ito, S., Flockerzi, V., Zhu, M. X., and Zholos, A. V. (2008) Isoform-specific inhibition of TRPC4 channel by phosphatidylinositol 4,5-bisphosphate. *J. Biol. Chem.* **283,** 10026–10036
43. Rohacs, T. (2007) Regulation of TRP channels by PIP(2). *Pflugers Archiv* **453,** 753–762
44. Dong, X. P., Shen, D., Wang, X., Dawson, T., Li, X., Zhang, Q., Cheng, X., Zhang, Y., Weisman, L. S., Delling, M., and Xu, H. (2010) PI(3,5)P(2) controls membrane trafficking by direct activation of mucolipin Ca(2+) release channels in the endolysosome. *Nature Commun.* **1,** 38
45. van Rossum, D. B., Patterson, R. L., Sharma, S., Barrow, R. K., Kornberg, M., Gill, D. L., and Snyder, S. H. (2005) Phospholipase Cgamma1 controls surface expression of TRPC3 through an intermolecular PH domain. *Nature* **434,** 99–104
46. Nilius, B., Owsianik, G., and Voets, T. (2008) Transient receptor potential channels meet phosphoinositides. *EMBO J.* **27,** 2809–2816
47. Errasti-Murugarren, E., Casado, F. J., and Pastor-Anglada, M. (2010) Different N-terminal motifs determine plasma membrane targeting of the human concentrative nucleoside transporter 3 in polarized and nonpolarized cells. *Mol. Pharmacol.* **78,** 795–803
48. Votsmeier, C., and Gallwitz, D. (2001) An acidic sequence of a putative yeast Golgi membrane protein binds COPII and facilitates ER export. *EMBO J.* **20,** 6742–6750

49. Zuzarte, M., Rinné, S., Schlichthörl, G., Schubert, A., Daut, J., and Preisig-Müller, R. (2007) A di-acidic sequence motif enhances the surface expression of the potassium channel TASK-3. *Traffic* **8,** 1093–1100
50. Nishimura, N., Plutner, H., Hahn, K., and Balch, W. E. (2002) The delta subunit of AP-3 is required for efficient transport of VSV-G from the trans-Golgi network to the cell surface. *Proc. Natl. Acad. Sci. U. S. A.* **99,** 6755–6760
51. Nishimura, N., Bannykh, S., Slabough, S., Matteson, J., Altschuler, Y., Hahn, K., and Balch, W. E. (1999) A di-acidic (DXE) code directs concentration of cargo during export from the endoplasmic reticulum. *J. Biol. Chem.* **274,** 15937–15946
52. Nishimura, N., and Balch, W. E. (1997) A di-acidic signal required for selective export from the endoplasmic reticulum. *Science* **277,** 556–558
53. Patterson, R. L., van Rossum, D. B., Ford, D. L., Hurt, K. J., Bae, S. S., Suh, P. G., Kurosaki, T., Snyder, S. H., and Gill, D. L. (2002) Phospholipase C-γ is required for agonist-induced Ca^{2+} entry. *Cell* **111,** 529–541
54. Nishida, M., Sugimoto, K., Hara, Y., Mori, E., Morii, T., Kurosaki, T., and Mori, Y. (2003) Amplification of receptor signalling by Ca2+ entry-mediated translocation and activation of PLCγ2 in B lymphocytes. *EMBO J.* **22,** 4677–4688
55. Lemmon, M. A. (2005) Pleckstrin homology domains: two halves make a hole? *Cell* **120,** 574–576